# Design and Testing of a Surgical Instrument to Measure Sternal Force During Treatment of Pectus Excavatum

Tiffany S. Liao & Aubrey A. Little

Yale University

Submitted in Fulfillment

Of the Requirements of the Degree of

*Bachelor of Science (BS) in Biomedical Engineering*

May 10, 2022

Mentors: Daniel Wiznia, MD and Steven Tommasini, PhD

# DESIGN AND TESTING OF A SURGICAL INSTRUMENT TO MEASURE STERNAL FORCE DURING TREATMENT OF PECTUS EXCAVATUM

Tiffany S. Liao & Aubrey A. Little (BME ‘22)

## ABSTRACT

This paper presents a modified design of the Pectus Flipper manufactured by Zimmer Biomet, used in the surgical treatment of pectus excavatum (PE), a chest wall condition where the sternum is depressed. Treatment involves surgically inserting a curved metal bar through the chest and underneath the sternum to elevate it to a normal position. The proposed modification of the Pectus Flippers used to flip the Nuss bar into position involves an additional side loft and socket to allow for torque wrench attachment. Conversion of torque to force allows for standardized measurement of the downward force of the chest on the Nuss bar and ribs. This measurement can help surgeons make real-time treatment decisions in the operating room, such as inserting additional bars or removing excess cartilage. Virtual and in-lab tests support the mechanical strength and durability of both the Pectus Flipper and the socket where the flipper and torque wrench interact. Virtual testing was completed through Solidworks FEA analysis, and a series of mechanical tests were performed using a hydraulic press. Validation testing in the lab resulted in measurements that are predictive of applied force. The Pectus Flipper - torque wrench measurement system produced precise force measurements that were consistent across tests performed with a hydraulic press and separate chest model of PE. This simple instrument design is feasible to use in the operating room and has the potential to create a new standardized method of determining treatment for PE patients, thereby reducing complications and improving patient outcomes.

## INTRODUCTION

### Background

Pectus excavatum (PE) is a deformity of the chest in which the sternum is depressed inward. PE is present in around 1 of every 400 live births and is three to five times more likely in males than females (Mayer Jan 2020). While there is no definitive cause for such deformities, it is speculated that defective cartilage growth and associated genetic factors increase the risk of PE. Additionally, the condition is associated with connective tissue disorders and neuromuscular diseases such as spinal muscular atrophy. PE develops in individuals at different ages, with only one-third of cases being present at infancy and the other two-thirds developing or worsening later in life, particularly during the years of adolescent growth spurts (Mayer Jan 2020).

While there are no severe debilitations or deaths directly associated with PE, the condition can negatively impact an individual's life. For example, cosmetic concern over physical appearance negatively impacts self-confidence and mental health. It has been shown that this concern subsides over time, but it remains the most common reason to seek surgical treatment. Other effects and associated prevalences are as follows: exercise intolerance (82%), chest pain (68%), poor endurance (67%), pulmonary function abnormalities (<33%), and cardiovascular dysfunction (30%), and shortness of breath (2%) (Mayer Jan 2020 and Raggio 2020).

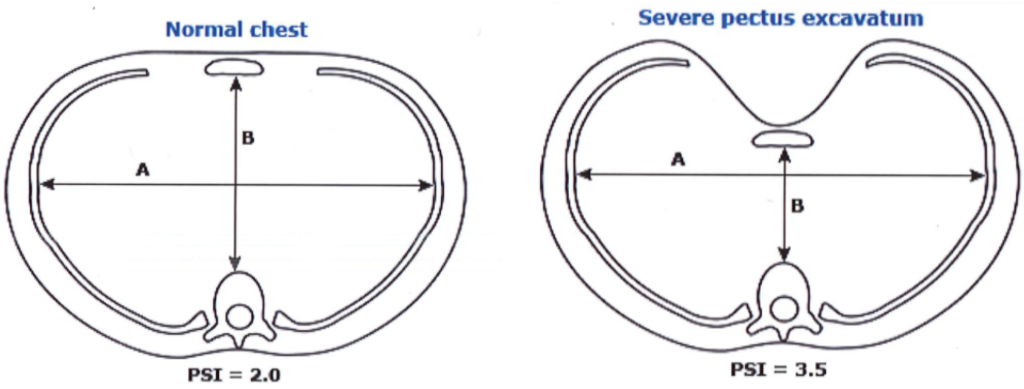


Figure 1. Calculation of Haller Index in a normal (left) and PE (right) CT of the chest.

Severity of PE is currently evaluated using the standardized Pectus Severity Index (PSI), also referred to as the Haller Index. It is calculated from the “ratio of transverse thoracic diameter to [the] diameter at maximal sternal depression” (Mayer Jan 2020). A normal PSI falls under 2.5, while a PSI from an individual with severe PE exceeds 3.25 (Figure 1). Upon evaluating the severity of the defect, the patient’s age, and functional testing results, the physician may encourage surgical treatment. Surgery is often performed in late childhood (>8 years) or early adolescence. Individuals within this age range are simultaneously young enough to have sufficient costal cartilage compliance to allow for adjustment and old enough so their cartilages will not regress during a growth spurt (Mayer Jan 2020).

**Treatment**

The most common reconstructive surgery for PE is the Nuss procedure. The surgery involves inserting a custom-contoured steel bar to elevate the sternum. First, the surgeon creates a substernal tunnel from one side of the chest to the other, using a scope to visualize the process. The Nuss bar is then pulled through this tunnel, passing behind the sternum and in front of the heart. The bar is inserted in a convex orientation. In order to rotate the bar into the correct concave orientation, Pectus Flippers are temporarily attached to either end of the bar and rotated by 180 degrees, allowing the bar to push out the sternum. The bar is typically supported by two ribs on each side of the chest for better load distribution. The Pectus Flippers are subsequently removed and absorbable stitches, heavy sutures, and a stabilizer are used to keep the bar in place. If the bar is not stabilized correctly, it can rotate about an axis and cause internal damage. Three of the most common types of bar displacement include “bar flipping” where the bar is rotated along a hinge axis, “lateral sliding” where the bar slips horizontally to one side due to asymmetric PE, and “hinge-point disruption” which is a dorsal shift of the bar due to intercostal musculature tear (Park et al. 2008). Although complications due to bar displacement have

decreased to 1.2% of cases, it still remains one of the most common types of postoperative complications (Saco 2019 and Garzi et al. 2020). If too much force is placed on one bar, there are increased chances of displacement and patient pain. This is common in adults as they tend to have stiffer cartilages and higher failure rates than adolescents. Furthermore, individuals with pre-existing conditions such as connective tissue diseases or asymmetric defects have increased risk of bar displacement due to potential atypical loading to the bar.

After around 2-3 years of treatment, the bar can be removed. Currently, the Nuss procedure leads to an average PSI decrease of 1.4 (Mayer Jue 2020). Some studies demonstrate an improvement in forced vital capacity (FVC) and other pulmonary functions, though this is still currently debated. In severe cases, including those with asymmetry, the surgeon may consider adding a second bar for additional stabilization. Another option for increasing stabilization and reducing pressure on the bar, particularly in adults who have stiffer cartilage, is the modified Ravitch procedure. This procedure involves removing small sections of the rib and subperichondrial cartilage in order to unload the sternum.

**Problem Statement / Prior Art / Approach**

The surgical approach to treating PE depends largely on the surgeon's preference and experience. Decisions that surgeons often face in the operating room are whether or not to add a second bar and/or remove cartilage. Surgeons take into consideration the patient's age, Haller index, and most importantly, the force necessary to pull up the sternum which is currently a subjective measurement. On one hand, a second bar may be necessary to help better distribute the pressure, thus preventing bar displacement and failure. On the other hand, inserting another bar takes an additional hour in surgery and introduces yet another foreign body into the host, increasing postoperative pain and chance of infection. The decision regarding cartilage removal should also factor in the risk of additional incisions and post-operative growth complications.

It is clear that surgeons treating PE patients clearly lack a standardized guide to treatment. Quantitative measurements of sternal force would help guide treatment decisions in the operating room, particularly in regards to the number of inserted bars (as discussed previously). This would benefit not only PE patients but surgeons as well by minimizing the use of a second bar, time in the operating room, and pain from the procedure.

Previous attempts to measure the force of the chest in PE have required invasive incisions and additional surgical steps. For example, Forkalsrud et al. attempted to determine chest force by using a hook-scale system to lift the sternum upward (Fonkalsrud). Other attempts to measure chest force include Alexander Tulenko's patented invention involving a sensor on a long rod inserted into the side of the chest and directly under the sternum to measure force (Tulenko). This invention was patented in 2017, although it is unknown if or where this device has been implemented. While useful, it does require an extra incision in the patient's chest, along with the insertion of an external device to high-risk areas in the chest (close to the heart).

The ultimate goal is to create a novel, noninvasive medical instrument to measure sternal force in the operating room. During the standard Nuss procedure, two Pectus Flippers are attached to each end of the curved bar after the bar has been inserted in concave orientation in the chest. The Pectus Flippers are used to flip the bar into its correct convex orientation. Standard stainless steel Pectus Flippers, such as those manufactured by Zimmer Biomet, include a slot for bar insertion, a vertically lofted neck portion, and a handle on the distal end (Figure 2a). Figure 2b below illustrates the interactions and forces between the sternum, bar, and Pectus Flippers during the procedure.

Figure 2a Pectus Flipper (Zimmer Biomet)

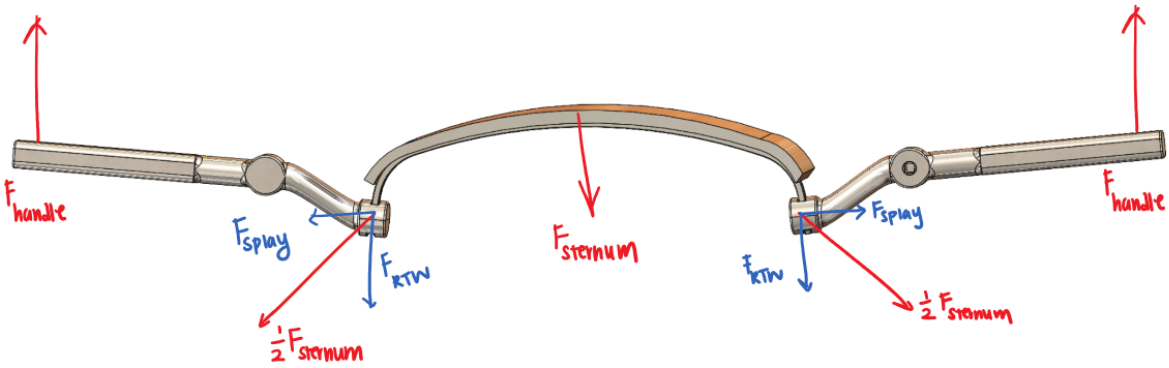


Figure 2b Free body diagram of the sternum. The components are as follows: sternum (reflected by the flat curved piece), Nuss bar (underneath the sternum), and the attached Pectus Flippers (at both ends of the Nuss bar). F_sternum is the force of the sternum on the bar. This force is then split as ½ F_sternum vectors angled outwards at the contact point between bar and Pectus Flipper due to “splaying.” The curvature of the bar produces a “splaying” effect upon the lifting of the Pectus Flipper handle. Therefore, as marked above, part of the force is distributed horizontally (F_splay) and is not accounted for by F_RTW (the force reading on the torque wrench), leaving the sum of the forces from the torque wrench readings to be less than the total force of the sternum. The F_handle force vectors reflect the upward forces on the Pectus Flipper that counteract F_sternum as the handles are simultaneously lifted. Ideally, barring any extraneous factors, the two F_handle forces should add up to F_sternum.

## METHODS AND RESULTS

### Ideation and Concept Design

Towards the beginning of the project, a few different options for tackling how to accurately produce real-time force measurements in the chest were debated. Some initial thoughts included utilizing a scale device (similar to Forkalsrud et al.) to measure force from the

center of the chest. Again, however, this is a high risk procedure that requires an extra incision in the middle of the chest, making it not only inconvenient but cosmetically suboptimal as well. Another design consideration involved using force sensor pads placed on the introducer that carves a tunnel for the bar. Unfortunately, this would not be effective as the sword is inserted in an incorrect orientation – concave up. Furthermore, there would be added risk of the sensor pads potentially slipping or falling into high-risk areas of the chest cavity during the procedure. One final consideration involved adding sensors to the Nuss bar to measure the forces between the sternum and the bar once the bar is inserted into the chest cavity. Once again, there would be added risk because the sensors are inserted into the body. Furthermore, the sensors are also not accurate over long periods of time or reposable.

After a live Nuss procedure observation, details regarding the surgical workflow and bar insertion were noted. The procedure required positioning the bar incredibly close to the heart, further confirming concerns with inserting additional instruments or devices through the chest. The chosen modified Pectus Flipper design is a non-invasive solution that also allows for asymmetry detection. It does not require additional incisions or disrupt the workflow of the procedure, simply adding to a predicate device already utilized in the procedure.

Upon 3D printing the first iteration modified Pectus Flipper, preliminary mechanical validation testing with a manual torque wrench was performed to ensure the prototype's ability to measure forces precisely (Figure 3). Using a scale and a make-shift Nuss bar, as well as a heavy stand, torque measurements were taken, converted to force, and compared to the actual force readings from the scale as shown below. Results show a 2% difference between the torque reading and scale reading. This validated the concept and from there, further mechanical properties testing was conducted before the design process was iterated to come to the current carbon fiber-reinforced Pectus Flipper prototype.

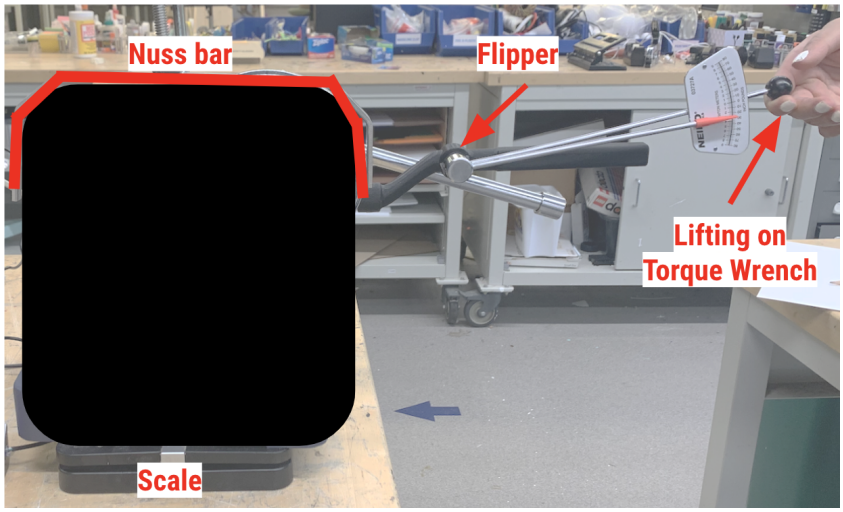


Figure 3. Preliminary mechanical validation testing of Pectus Flipper-torque wrench combination utilizing a lift-up technique to ensure device ability to measure forces.

The modified Pectus Flipper allows for torque wrench attachment and subsequent measurement of sternal force on the Nuss bar (Figure 4). Each Pectus Flipper is given an additional loft to the right side to allow for torque wrench insertion in line with the Nuss bar, simplifying the torque to force conversion. A rectangular socket is formed on the left side of the device at the base of the neck to allow for torque wrench attachment. The torque wrench ratchet head will slide into this socket, allowing for proper interaction between the Pectus Flipper and torque wrench while the right side loft will keep it in line with the Nuss bar. When lifting the torque wrench alone, the attached Pectus Flipper will also lift in conjunction. The torque wrenches are to be lifted at the same time so the Nuss bar is just hovering over the ribs (~2cm) but not touching them. This allows for an accurate conversion of the torque reading to a chest-on-bar force measurement. The measurement is taken before the bar is tied to the ribs. Eventually, the goal is for surgeons to be able to enter the torque readings into a database that will recommend treatment based on personalized patient information using a machine learning algorithm.

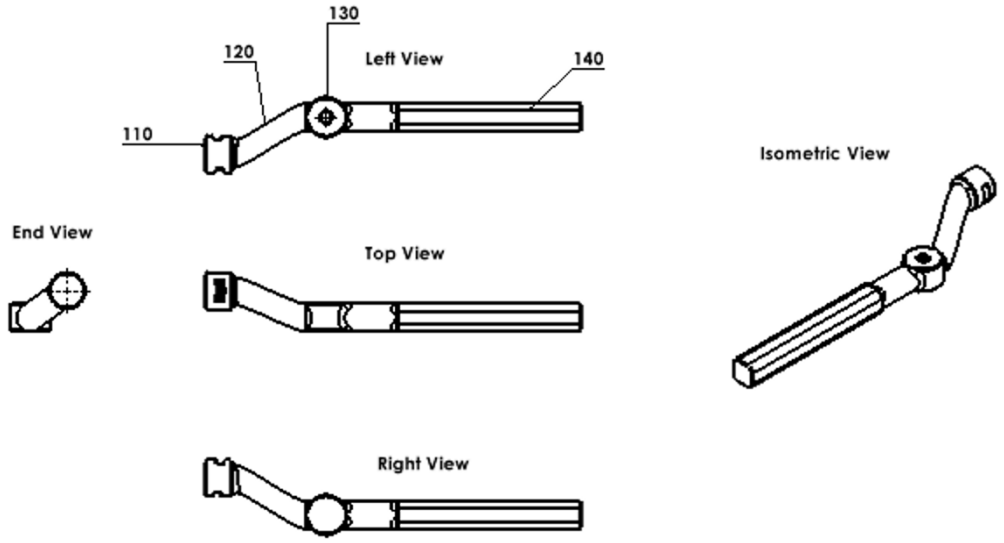


Figure 4. Drawings of modified Pectus Flippers. The side loft can be seen from the top view, while the additional slot can be seen from the left view (130). Both can be seen in the isometric view.

The modified Pectus Flippers used for mechanical testing were initially 3D printed from polylactic acid (PLA). The initial prototype, which we will refer to as the Modified Original Pectus Flipper, was a 3D-printed, double-lofted Pectus Flipper with an added socket for the insertion of the torque wrench, as shown in Figure 5a. In order to create a device more similar in strength and function as a stainless steel manufactured Pectus Flipper, a new iteration prototype was created with emphasis on reinforcing the two most important load points on the device: 1. the neck and 2. Pectus Flipper - torque wrench interaction socket. FEA analysis confirmed the stress concentration at these points. The double loft creates a slightly weakened neck region where the majority of the sternum's force (and the force due to splaying) is concentrated. Therefore, carbon fiber reinforcements were introduced in every 5 layers of PLA using Eiger software, with a 45 degree rotation after every layer so the fibers lay in a multidirectional manner, thereby increasing the strength (Figure 5b). Additionally, a metal insert was added

inside the socket on the Pectus Flipper, allowing for a more accurate simulation of the metal-on-metal interaction between a true Pectus Flipper and torque wrench. Aluminum square tubing was used to create the insert. This current prototype will be referred to as the Carbon Fiber-Reinforced Pectus Flipper.

Figure 5a: Carbon fiber-reinforced Pectus Flipper with a metal insert.

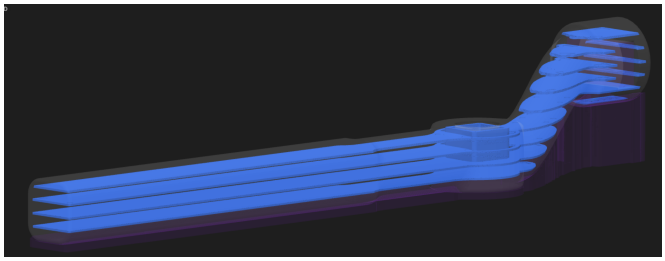

Figure 5b: Carbon fiber reinforcements were introduced in every 5 layers. (Software: Eiger)

**FEA Analysis**

Finite element analysis (FEA) fatigue testing and cyclic loading simulations were performed on the modified Pectus Flippers to ensure non-failure. A Solidworks model of the Pectus Flipper was made to scale and attached to a GrabCad model torque wrench.

The constraints used for simulation were as follows: the torque wrench was fixed in place to simulate its use in the operating room. A simple contact was introduced in Solidworks between the Pectus Flipper and torque wrench. A downward force was then applied to the distal portion of the Pectus Flipper where the Nuss bar inserts into the slot. Gravity was included for a more accurate simulation.

The forces applied on the distal ends of the Pectus Flipper were 10N, 50N, and 150N. Upon analysis, it is clear the stress is concentrated around the neck and socket of the Pectus Flipper (as shown in Figure 6a). The resulting maximum von Mises stress and displacement measurements are summarized in Table 1. The displacement for all forces is negligible.

Table 1. Solidworks simulation results. Values are reported for the maximum stress and displacement felt on the Pectus Flipper - torque wrench combination in response to increased applied force.

| Force Exerted | Max Von Mises Stress | Displacement |
|---|---|---|
| 10N | $3.381 \times 10^4$ N/m^2 | $2.397 \times 10^{-5}$ mm (~0) |
| 50N | $1.014 \times 10^5$ N/m^2 | $8.216 \times 10^{-5}$ mm (~0) |
| 150 N | $5.072 \times 10^5$ N/m^2 | $4.104 \times 10^{-4}$ mm (~0) |

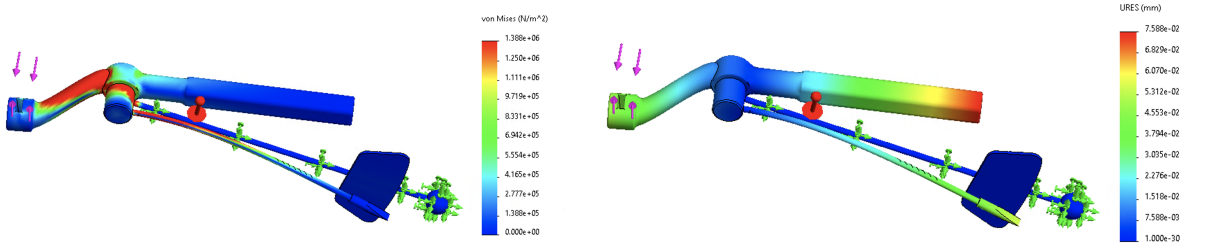


Figure 6. a) Stress results and b) displacement results of FEA analysis of 150N load placed on a stainless steel Pectus Flipper - torque wrench combination.

Through a cyclic loading test on Solidworks, higher stress was found in the socket of the Pectus Flipper in comparison to the rest of the system once the torque wrench is inserted.

## Mechanical Testing

### Test 1: Stiffness / Strength of Modified Original Pectus Flipper

To test the stiffness and mechanical strength of the original 3D printed prototype, the following experimental setup was used (as shown in Figure 7a). The clamps stabilized the Pectus Flipper handle 6.8 centimeters from the proximal end. Additional clamps and wood

pieces were used to hold the system in place while the hydraulic press was aligned to contact the distal end of the Pectus Flipper (near the bar insertion slot). A downward force by the hydraulic press was applied at 5N and 10N intervals until the load curve began to flatten out (Figure 7b). The stiffness and yield load are 8.47 N/mm and 20.94 N, respectively.

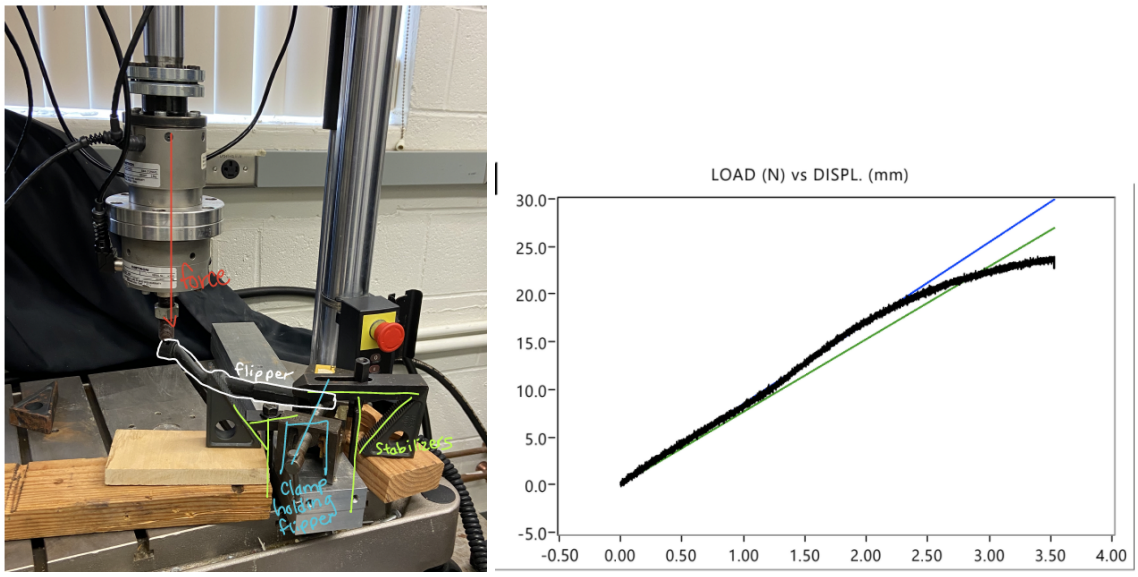


Figure 7. a) Experimental setup for testing the strength of the Modified Original Pectus Flipper prototype. Clamps were used to hold the Pectus Flipper in position while the hydraulic press applied increasing pressure in intervals to the proximal end of the Pectus Flipper. b) Load vs. Displacement curve for the Modified Original Pectus Flipper prototype.

**Test 2: Stiffness / Strength of the Carbon Fiber-Reinforced Pectus Flipper**

The strength of the Carbon Fiber-Reinforced Pectus Flipper was tested utilizing the same setup as before. The stiffness and yield load are 9.25 N/mm and 29.21 N, respectively (Figure 8). Table 2 displays the mechanical strength properties for both the original and carbon fiber reinforced Pectus Flippers. The carbon fiber reinforced Pectus Flippers are 9.2% stiffer than the regular 3D printed Pectus Flippers and have a 50% higher yield load, indicating a definitive increase in the strength of the device prototype.

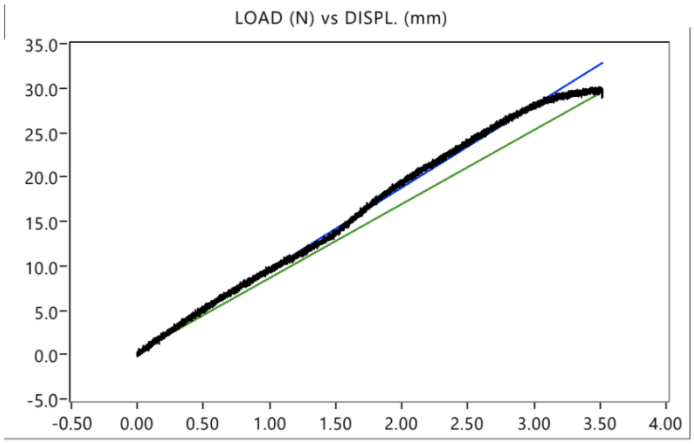


Figure 8. Load vs Displacement curve for the carbon-reinforced 3D-printed flipper.

Table 2. Comparison of mechanical strength properties of the original 3D-printed Pectus Flipper and the carbon fiber reinforced Pectus Flipper.

| **Stiffness Test Data** | | |
|---|---|---|
| | Modified Original Pectus Flipper | Carbon Fiber-Reinforced Pectus Flipper |
| Stiffness (N/mm) | 8.473 | 9.251 |
| Max Load (N) | 23.99 | 30.15 |
| Yield Load (N) | 20.94 | 29.21 |
| Yield Displacement (mm) | 2.756 | 3.486 |
| Work to Yield (Nmm) | 89.96 | 158.04 |

**Test 3: Strength Testing of Pectus Flipper - Torque Wrench Interaction**

A mechanical test was performed on the square socket of the Pectus Flipper - torque wrench interaction. The torque wrench was clamped in place from 3.4cm to 9.8cm from the circular end piece of the torque wrench. As before, the block-and-clamp system was used to stabilize the configuration, while the press was aligned with the distal end of the Pectus Flipper near the bar insertion slot (Figure 9a).

A load was applied to the end of the Pectus Flipper in increasing 5N and 10N intervals with the torque wrench clamped in place. Stiffness was calculated using the initial slope of the curve before the dip, which was caused by some shifting of materials (Figure 9b). The stiffness of the combined apparatus was found to be 10.286 N/mm, the yield stiffness was 9.26 N/mm, and even at the maximum load of 172 N, there was no device deformation or failure.

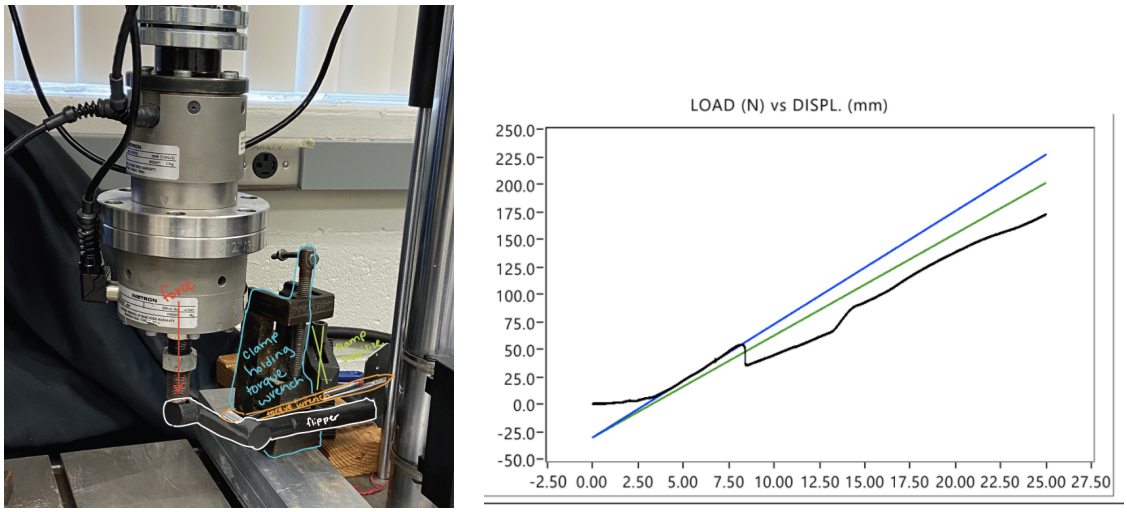


Figure 9. a) Experimental setup for testing the Pectus Flipper - torque wrench interaction. The torque wrench is inserted into the socket and clamped down by its handle. A load is applied to the distal end of the freely floating Pectus Flipper. b) Resulting Load vs. Displacement plot for the Pectus Flipper - torque wrench interaction.

## Test 4: Two-sided Validity Testing with Hydraulic Press

In order to validate the torque wrench outputs, both Pectus Flippers were attached to the ends of the 11.125-inch Nuss bar (Figure 10). The Nuss Bar was a sample Nuss Bar provided by Zimmer that had been bent into a convex shape so it would fit into a chest that was 9 inches across. Digital torque wrenches were inserted into the Pectus Flipper slots and clamped to the work bench. Digital torque wrenches were used in place of manual torque wrenches for this particular test in order to generate more precise values. Two assistants applied simultaneous downwards forces on the torque wrenches, translating into a force read by the hydraulic press contacting the Nuss bar. The force applied increased in intervals over time. The readings from

each torque wrench were recorded, as well as the total combined force felt by the hydraulic press. The resulting data from two trial runs are as follows.

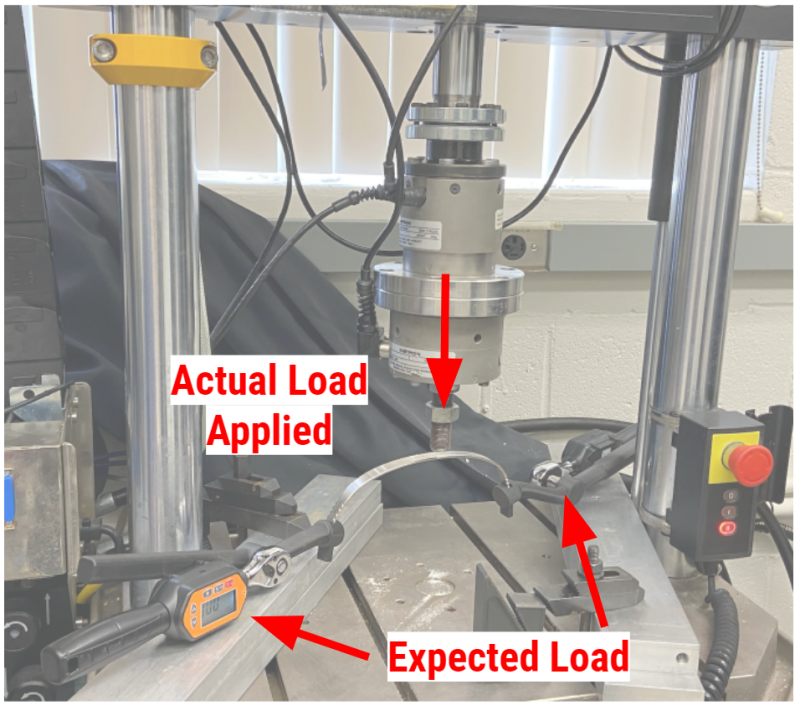


Figure 10. Experimental setup of the Nuss bar connected to two Pectus Flipper - torque wrench combinations on each side. Force was applied to the center of the bar, and the torque wrench readings were recorded.

The data collected are recorded in the following tables. “Actual Load” reflects the load reading from the Intron while the T1 and T2 indicate the torque readings from the left and right torque wrenches, respectively. The “Expected Load” is the total force calculated through manual conversion of the torque wrench readings to force. The conversion is done through dividing the torque by the distance between 1. the applied force on the Nuss bar and 2. the torque wrench - flipper combination on each side. The actual load versus the expected load for the two trials were plotted in Figure 11, and the slopes were 0.7848 and 0.7683, respectively. The $R^2$ values were 0.9942 and 0.9915, respectively, indicating a significant correlation between the expected and actual loads. The data also indicates the expected load (from manual conversion of the torque wrenches) was around 77.6% of the actual force read by the Intron. The dissipation of force here can be explained by the “splaying effect” illustrated in Figure 2.2, in which the force

applied directly to the Nuss bar does not directly translate to a vertical force at the ends of the Nuss bar due to the outward splay. Given the consistency of the slope across the wide range of applied forces, from 30 N to 173 N, the results of the data collection validate the feasibility and precision of the torque wrench readings.

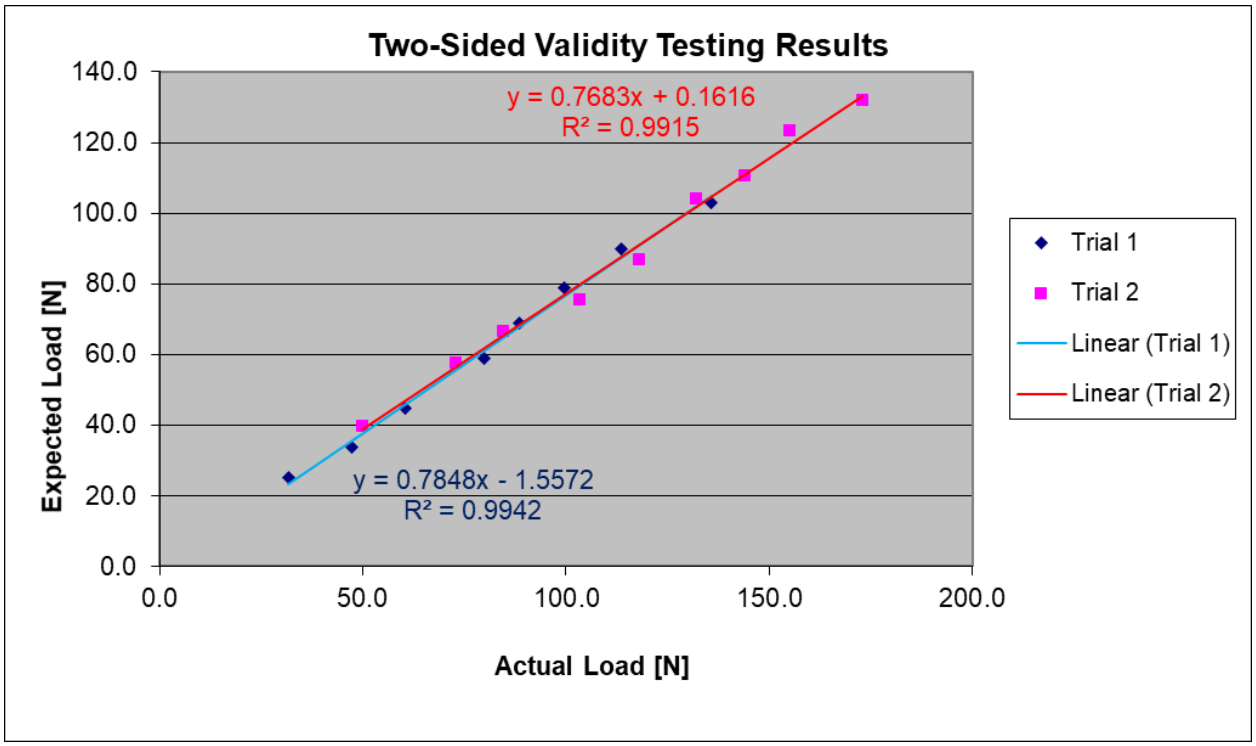


Figure 11. The expected load calculated from the two torque wrench readings plotted against the actual load that was applied using the hydraulic press. The expected load was ~77.6% of the actual force applied due to the force splaying effect of the bar. $R^2$ values above 0.99 indicate significant correlation and high precision of the system.

## Test 5: One-Sided Validity Testing in Chest Model

The next step was to validate the measurements within an Axis Scientific chest model purchased from Anatomy Warehouse. The model's cartilages were made of inflexible plastic and thus did not replicate the compliant behavior of the chest. Therefore, in order to generate the inward depression of the sternum for pectus excavatum, the sternum was cut in half and the depression was created on the left side of the chest through a combination of rubber bands and binder rings as shown in Figure 12b below.

Figure 12. a) One Axis Scientific chest model was purchased. b) In order to replicate the inward deformity of PE, the sternum was cut down the middle and the left side was pulled down with elastic rubber bands.

Similar to the two-sided validation test with the hydraulic press, direct force measurements were compared with torque-to-force conversions (Figure 13). Direct measurements of the force required to lift the depressed side of the chest up to level with the control side were taken with a luggage scale to measure the actual load. Then, the Nuss Bar was fed through the ribs and under the sternum. While manually fixing the end of the bar opposite of the depression, the Pectus Flipper - torque wrench combination was used to lift the bar and sternum to the level of the normal side of the chest. The torque wrench reading was recorded at this peak.

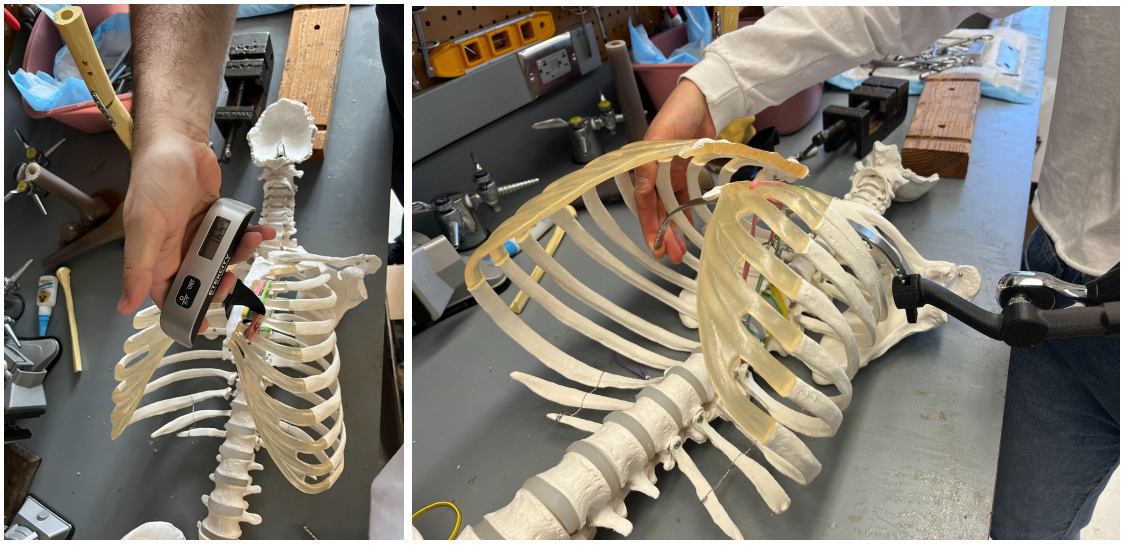

Figure 13. Measurement of chest force using a) A luggage scale and b) The flipper - torque wrench combination. The two measurements were compared to determine accuracy and precision.

Two trials were conducted. Five readings were averaged for each trial utilizing both the luggage scale and Pectus Flipper - torque wrench combinations. For the first trial, the luggage scale read a force of 15.8 lbs consistently, which converts to 70.3 N, representing the actual load. The measurements recorded utilizing the Pectus Flipper - torque wrench combination are shown in Table 3 below. The resulting average error between the torque-converted “expected” load and actual load for the five measurements was -37.1%, indicating the expected load was 37.1% lower than the actual force exerted.

Table 3. Testing data on chest model (Trial 1)

| **Luggage Scale Measurements** | | **Torque Wrench Measurement** | | | |
|---|---|---|---|---|---|
| Original (lb) | Force (N) | Torque reading (N*m) | Distance (m) | Force conversion (N) | % Error |
| 15.8 | 70.28 | 9.84 | 0.204 | 48.2 | -31.4 |
| 15.8 | 70.28 | 7.89 | 0.204 | 38.7 | -45.0 |
| 15.8 | 70.28 | 8.78 | 0.204 | 43.0 | -38.8 |
| 15.8 | 70.28 | 9.03 | 0.204 | 44.3 | -37.0 |
| 15.8 | 70.28 | 9.53 | 0.204 | 46.7 | -33.5 |

| **Average Error** | **-37.1** |
|---|---|

For the second trial, some rubber bands were loosened to decrease the force on the sternum. The same measurements (with a luggage scale and the Pectus Flipper - torque wrench combination) were taken and are shown in Table 4 below. The resulting average error between the torque-converted load and actual load for the five measurements was -34.6%, indicating the torque measurement was 34.6% lower than the actual force exerted.

Table 4. Testing data on chest model (Trial 2)

| **Luggage Scale Measurements** | | **Torque Wrench Measurement** | | | |
|---|---|---|---|---|---|
| Original (lb) | Force (N) | Torque reading (N*m) | Distance (m) | Force conversion (N) | % Error |
| 14.5 | 64.50 | 8.2 | 0.204 | 40.2 | -37.7 |
| 14.2 | 63.16 | 8.35 | 0.204 | 40.9 | -35.2 |
| 14.3 | 63.61 | 8.2 | 0.204 | 40.2 | -36.8 |
| 14.3 | 63.61 | 9.06 | 0.204 | 44.4 | -30.2 |
| 14.6 | 64.94 | 8.87 | 0.204 | 43.5 | -33.0 |

| **Average Error** | **-34.6** |
|---|---|

**Test 4 and 5 Summary**

The results from the validation testing with the hydraulic press and the chest model indicate precision in the measurements. The error was roughly 23% for the hydraulic press test and 35% for the chest model test. The splaying effect, as mentioned in the Test 4 section, can explain the *consistently* lower measurements resulting from the flipper - torque wrench combination. The range of error produced from the luggage scale is higher, around 35%, which could be due to human error when lifting on the torque wrench, not fully reaching the same elevation as the luggage scale due to physical strength constraints.

**Database and Machine Learning Model**

With the modified Pectus Flippers, surgeons are able to take force measurements during surgical procedures. A database must then be created to track treatment-results combinations for patients in a variety of different scenarios. Once substantial data is collected, a machine

learning algorithm can be developed to predict patient treatment. To initiate the software component of this project, a software development plan was created based on the suggestions from the following textbook: Introduction to Medical Software: Foundations for Digital Health, Devices and Diagnostics (Papademetris X., Quraishi A.N., and Licholai G.P. Cambridge University Press, 2022).

The intended users of this database are trained pediatric surgeons and assistants who perform PE surgeries. The intended use environment is the operating room. There are two primary intended uses of this database. The first is for doctors performing the surgery to document and record their decisions and the long-term results in order to contribute to the database of cases that will be used to create the database. As the database grows, the more accurate the machine learning model will be. The second use for the database is to provide inexperienced surgeons with reference points for their decisions when it comes to the treatment of pectus excavatum given a patient's particular circumstances.

The intended workflow would be as follows: Before surgery, the surgeon logs into his/her private account (Figure 14a). They will be directed to a screen asking them to classify their patient as old or new (Figure 14b). If he/she is operating on a returning patient (Figure 14c), then he/she can search for the patient in their database by using previous operation date, age and gender. If he/she is operating on a new patient (Figure 14d), he/she will input anonymized patient information, such as the date of surgery, age, gender, weight, Haller index, race, activity level, and other pre-existing health conditions.

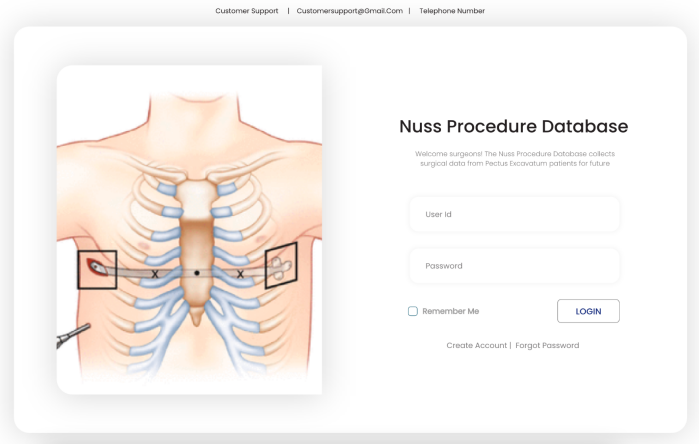


Figure 14a. Database login

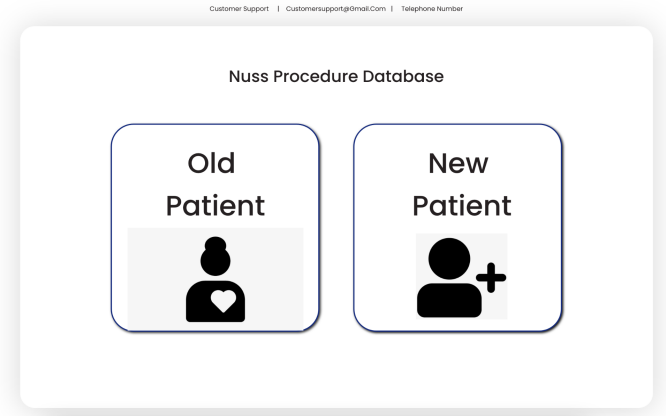


Figure 14b. Patient classification

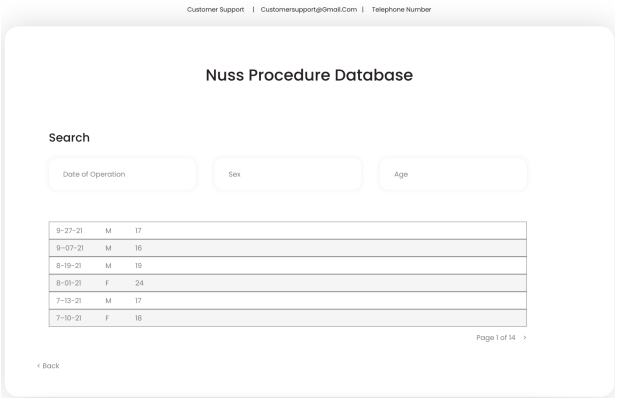


Figure 14c. Returning patient search page

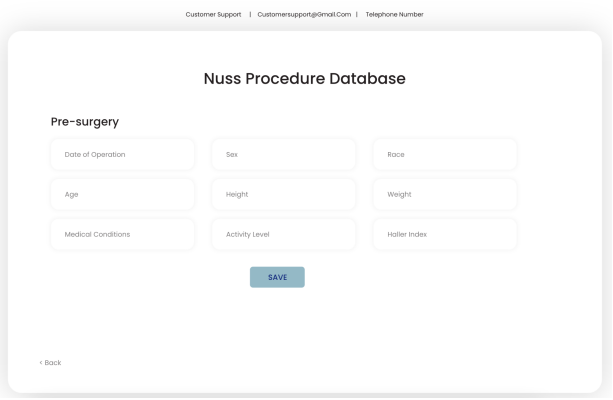


Figure 14d. New patient data form

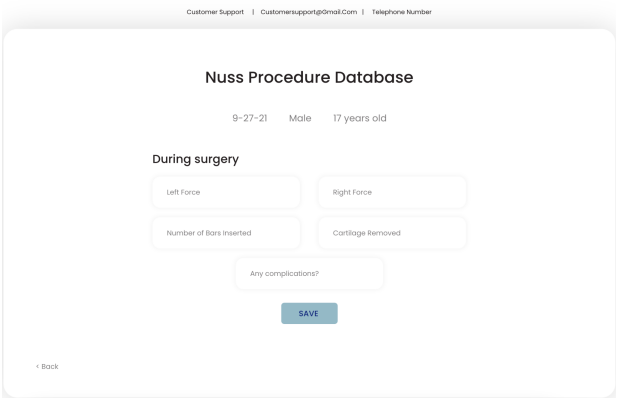


Figure 14e. Entering force data during surgery

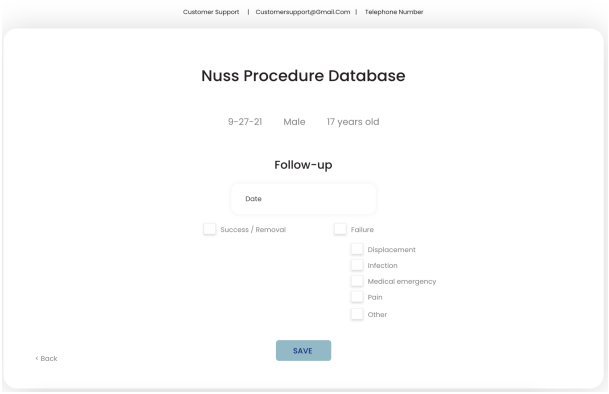


Figure 14f. Entering follow-up information

During surgery, while the surgeon is still logged in and has the patient information pulled up, he/she will measure the left and right forces using the torque wrenches. The measurements, along with the surgeon's treatment decision based on expert judgment, are input into the program (Figure 14e). For a returning patient, the surgeon must insert the date of bar removal and indicate successful or unsuccessful treatment (Figure 14f). The data collected by these expert surgeons will include patient factors, chest force, and surgical treatment. Upon more extensive data collection, a machine learning algorithm will be created from the dataset. This algorithm will be used to predict and recommend future treatments based on patient factors and chest forces.

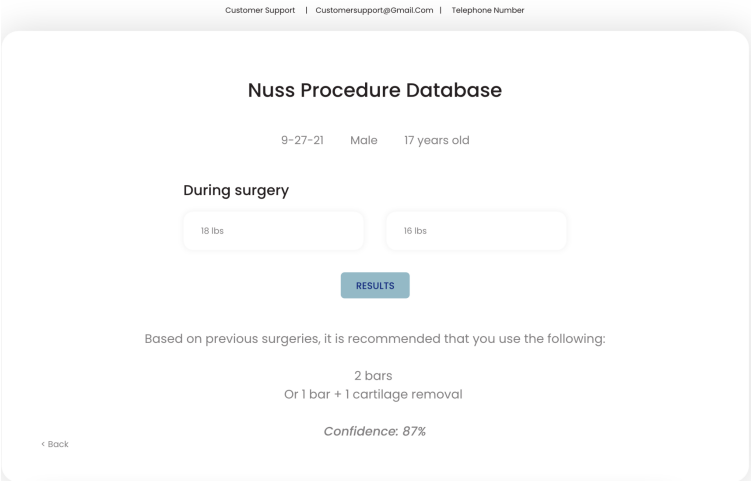

Figure 14g. Final database function - predicting treatment based on force measurements.

After sufficient data is acquired to develop a robust machine learning algorithm, the surgeons will see the screen above (Figure 14g), where they can input forces from both sides of the chest. The software will then output recommended treatment and confidence levels. The functionality of the software component is two-fold: first, it must safely store anonymized data and secondly, it must algorithmically determine the best treatment option given various parameters of the patient and chest forces.

In conducting risk analysis for this software, a few risks were identified. First, measures must be taken to ensure that the torque measurements are taken correctly and reported in the correct units. A checking mechanism could be implemented to ensure that the values fall within a physiological range. Another risk factor for any software with patient data is privacy protection. The data must be protected and only accessible to the associated physician. A password protected login and additional security measures should be implemented to protect patient information. Finally, the greatest risk for this type of machine learning application is providing recommendations that lead the surgeon astray. By including multiple treatment options and a confidence level, the surgeon can make his/her own calculated decision based on the recommendation of the software. Ideally, the software should reflect the decision of expert surgeons, and with this database structure, the algorithm will improve over time as more data is added. The algorithm should be utilized as a tool for the surgeon, not a replacement for their own decision-making.

## SIDE EXPERIMENT

Researchers from the Korea University College of Medicine developed a regression model that revealed certain factors (age, gender, depression angle, and depression depth) to be associated with double-bar insertion (Kim et al. 2015). Building on this finding, we developed

our own simplified machine learning (ML) model to predict surgical treatment of pectus excavatum. Specifically, a multiple regression model was constructed to predict the number of bars to be inserted. The inputs to the model include age, gender, and the following four measurements from CT scans illustrated in Figure 15: 1. Maximum transverse diameter (T), 2. Minimum anteroposterior (AP) distance (V), 3. Maximum depression distance (D), and Distance from maximum depression to maximum protrusion (G).

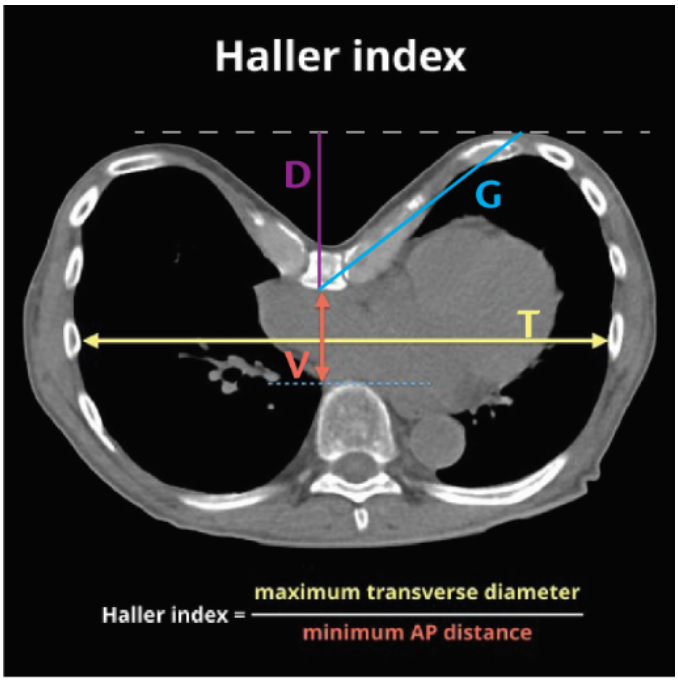


Figure 15. Four CT scan-derived measurements used as inputs in the regression model predicting PE treatment.

80% of CT scans were used for training and 20% of scans were used for testing. Due to IRB constraints on patient data, we were unable to collect a sufficient number of scans for a representative sample. Thus, the model is limited by the extremely small sample size; however, it is presumed that with more data, this model could become the first available accurate and noninvasive tool for presurgical planning of PE.

## CONCLUSION

The novel redesign of the Pectus Flipper offers a useful way to measure the force of the chest during surgical treatment of pectus excavatum (PE). The alterations made on a predicate device, along with minimal disruption to the procedure workflow support the feasibility of this surgical instrument. Virtual and in-lab mechanical testing further support the mechanical strength and durability of both the Pectus Flipper and the Pectus Flipper - torque wrench system. Validation testing in the lab resulted in precise measurements predictive of applied force.

While the data and experiments prove the feasibility and validity of the modified Pectus Flippers, there are a few limitations to its application in the operating room. In particular, the torque wrenches are clunky and can not be cleaned, meaning they must be wrapped in plastic to maintain sterility. Furthermore, clinical testing in the operating room is needed to determine the precision of the device in measuring chest forces in individuals with asymmetric chest structures, among other unique cases. Once ample data is collected to create a database of chest measurements and treatment results, a regression model may be created to assist surgeons in predicting the best path forward for treatment. It is possible that the model will not be predictive of treatment; however, based on current treatment decisions and imaging methods, it is reasonable to believe that the forces measured from the chest will be useful in differentiating between surgical decisions.

## FUTURE DIRECTIONS

Future directions for this project include, but are not limited to, developing the database, manufacturing the prototype, running clinical tests, generating the machine learning model, and evaluating the usefulness of the final product and software based on testing results. Future iterations of the project could be predictive of other aspects of the surgery, such as bar placement or duration of bar insertion.

The simple and innovative modification to the Pectus Flipper benefits multiple parties. For the surgeon, it allows for an efficient way to obtain a critical measurement early on in the procedure that can guide the rest of the operation and reduce uncertainty. In the long term, the data collected in regards to the force measurements for different patients with different treatment variations will assist in the creation of a standardized procedure for all surgeons. Furthermore, the device will benefit patients and hospitals by decreasing operation and recovery time as well as the number of re-surgeries. With continuous data collection over time, surgeons will have a better sense of what type of patient needs a second bar (or third), thereby minimizing the use of additional bar(s) in surgical procedures.

The benefit of our device will hopefully extend beyond the realm of PE, with applications in all types of surgeries from knee and hip arthroplasty to other procedures requiring force measurements pre-, during or post-operation. This also includes pectus carinatum, the opposite of pectus excavatum. In a broader sense, the process of personalizing medicine (such as predicting treatment based on a machine learning model) holds great potential for surgical outcomes and the medical field as well.

**ACKNOWLEDGEMENTS**

Since the start of the design process, we have collaborated with Dr. Michael Caty at Yale New Haven Hospital. Dr. Caty first proposed the clinical problem, provided background on PE treatment, and explained the current treatment process from the surgeon's point of view. He also provided opportunities for clinical and surgical observation. Our principal investigators, Dr. Wiznia and Dr. Tommasini (Yale BME) have provided guidance and suggestions throughout the process as well, with Dr. Tommasini being heavily involved in the mechanical testing of the prototype and Dr. Wiznia helping us understand the mechanics of the device. Peter Torab and Nicholas Bernardo (Yale SEAS) have been helpful in the process of design iteration and prototype creation. Gregory Roytman, a postdoctoral associate at the School of Medicine has helped in a variety of ways as well, from FEA analysis to mechanical testing. We have also spoken to other experts in the PE field including Dr. Robert Obermeyer, Dr. Robert Kelly, and Dr. Mohammad Obeid (Children's Hospital of The King's Daughters), who have given us feedback on our design and suggested next steps. Finally, Dr. Xenophon Papademetris (Yale BME) and Dr. Obeid have provided insight particularly on the software component of the project.

**REFERENCES**

*3 Advancements in Surgical Instruments*. (n.d.). Solvay. Retrieved April 13, 2021, from https://www.solvay.com/en/chemical-categories/specialty-polymers/healthcare/surgical-devices/3-advancements-in-surgical-instruments

Bauerfeind Hans, HB. (2021). Pad Comprising a Pressure Element. (Germany Patent No. WO2021037789 (A1)). European Patent Office.

Betti, S., Ciuti, G., Ricotti, L., Ghionzoli, M., Cavallo, F., Messineo, A., & Menciassi, A. (2014). A Sensorized Nuss Bar for Patient-Specific Treatment of Pectus Excavatum. *Sensors (Basel, Switzerland)*, *14*(10), 18096–18113. https://doi.org/10.3390/s141018096

Cierpikowski, P., Rzechonek, A., Błasiak, P., Lisowska, H., Pniewski, G., & Le Pivert, P. (2018).

Surgical Correction of Pectus Excavatum by the Nuss Procedure: A 15-Year Experience Study. Advances in experimental medicine and biology, 1047, 31–40. https://doi.org/10.1007/5584_2017_121

Fonkalsrud EW, Reemtsen B. Force required to elevate the sternum of pectus excavatum patients. J Am Coll Surg. 2002 Oct;195(4):575-7. doi: 10.1016/s1072-7515(02)01245-0. PMID: 12375767.

Frost & Sullivan (2020). 'GROWTH OPPORTUNITIES IN IMPLANTABLE SENSORS, LIDAR, HVAC PRESSURE SENSORS, AND WEATHER STATION'. Available at: https://cds-frost-com.yale.idm.oclc.org (Accessed: 9 April 2021).

Garzi, A., Prestipino, M., Rubino, M. S., Di Crescenzo, R. M., & Calabrò, E. (2020). *Complications of the "Nuss Procedure" In Pectus Excavatum.* Translational Medicine @ UniSa, 22, 24–27.

IBISWorld (2019). 'Pressure Sensor Manufacturing'. Available at: https://my-ibisworld-com.yale.idm.oclc.org/us/en/industry-specialized/od5384/about (Accessed: 9 April 2021).

Jaroszewski, D. E., Ewais, M. M., Chao, C. J., Gotway, M. B., Lackey, J. J., Myers, K. M., Merritt, M. V., Sims, S. M., McMahon, L. E., & Notrica, D. M. (2016). Success of Minimally Invasive Pectus Excavatum Procedures (Modified Nuss) in Adult Patients (≥30 Years). The Annals of thoracic surgery, 102(3), 993–1003. https://doi.org/10.1016/j.athoracsur.2016.03.105

Kim, H. C., Park, H. J., Nam, K. W., Kim, S. M., Choi, E. J., Jin, S., Lee, J.-J., Park, S. W., Choi, H., & Kim, M. G. (2010). *Fully automatic initialization method for quantitative assessment of chest-wall deformity in funnel chest patients.* Medical & Biological Engineering & Computing, 48(6), 589–595. https://doi.org/10.1007/s11517-010-0612-3

Kim, H. C., Park, M. S., Lee, S. K., Nam, K. C., Park, H. J., Kim, M. G., Song, J.-J., & Choi, H. (2015). *Normalized mean shapes and reference index values for computerized*

*quantitative assessment indices of chest wall deformities.* Journal of the Korean Physical Society, 67(10), 1868–1875. https://doi.org/10.3938/jkps.67.1868

Kim, K. H., Lee, K. Y., Lee, J. B., Yang, K.-S., Hwang, J., Je, B. K., & Park, H. J. (2015). Radiologic factors related to double-bar insertion in minimal invasive repair of pectus excavatum. World Journal of Pediatrics, 11(2), 148–153. https://doi.org/10.1007/s12519-014-0522-9

Mayer, O. H., MD. (2020, January 21). Pectus excavatum: Etiology and evaluation. Retrieved April 9, 2021, from https://www.uptodate.com/contents/pectus-excavatum-etiology-and-evaluation

Mayer, O. H., MD. (2020, June 15). Pectus excavatum: Treatment. Retrieved April 9, 2021, from https://www.uptodate.com/contents/pectus-excavatum-treatment

Nakagawa, Y., Uemura, S., Nakaoka, T., Yano, T., & Tanaka, N. (2008). *Evaluation of the Nuss procedure using pre- and postoperative computed tomographic index.* Journal of Pediatric Surgery, 43(3), 518–521. https://doi.org/10.1016/j.jpedsurg.2007.10.033

Nasr, A., Fecteau, A., & Wales, P. W. (2010). Comparison of the Nuss and the Ravitch procedure for pectus excavatum repair: A meta-analysis. *Journal of Pediatric Surgery*, *45*(5), 880–886. https://doi.org/10.1016/j.jpedsurg.2010.02.012

Obeid, M. F., Kelly, R., & McKenzie, F. D. (2021). *Development and Validation of a Hybrid Nuss Procedure Surgical Simulator and Trainer.* IEEE Transactions on Bio-Medical Engineering, 68(8), 2520–2528. https://doi.org/10.1109/TBME.2020.3048516

Papademetris, X., Quraishi, A. N., & Licholai, G. P. (2022). Introduction to medical software: Foundations for Digital Health, devices, and Diagnostics. Cambridge University Press.

Park, H. J., Chung, W.-J., Lee, I. S., & Kim, K. T. (2008). *Mechanism of bar displacement and corresponding bar fixation techniques in minimally invasive repair of pectus excavatum.*

Journal of Pediatric Surgery, 43(1), 74–78. https://doi.org/10.1016/j.jpedsurg.2007.09.022

Raggio, I. M., Martínez-Ferro, M., Bellía-Munzón, G., Capunay, C., Munín, M., Toselli, L., Carrascosa, P., & Rodríguez-Granillo, G. A. (2020). Diastolic and Systolic Cardiac Dysfunction in Pectus Excavatum: Relationship to Exercise and Malformation Severity. *Radiology: Cardiothoracic Imaging*, *2*(5), e200011. https://doi.org/10.1148/ryct.2020200011

Sacco Casamassima MG, Goldstein SD, Salazar JH, McIltrot KH, Abdullah F, Colombani PM. Perioperative strategies and technical modifications to the Nuss repair for pectus excavatum in pediatric patients: a large volume, single institution experience. J Pediatr Surg. 2014 Apr;49(4):575-82. doi: 10.1016/j.jpedsurg.2013.11.058. Epub 2013 Nov 27. PMID: 24726116.

Schwabegger, A. H., Del Frari, B., & Metzler, J. (2017). Technical consideration of the MOVARPE technique in intricate pectus excavatum deformity. *Wiener Klinische Wochenschrift*, *129*(19), 702–708. https://doi.org/10.1007/s00508-017-1214-y

Tulenko Alexander, AT. (2017). Nuss Procedure Aid.

(USA Patent No. US010376295). United States Patent and Trademark Office.

Wang, H., Liu, W., Zhang, D.-Y., Si, W.-Y., Yang, Q.-L., Lu, L.-W., Wang, F.-H., Li, L., Wang, Q., & Xia, H.-M. (2021). *Surface topography index: A novel deformity severity assessment index for pectus excavatum.* Translational Pediatrics, 10(8), 2044–2051. https://doi.org/10.21037/tp-21-282

Yock, P. G., & Zenios, S. (2020). Biodesign: The process of Innovating Medical Technologies. Cambridge University Press.